THE ASTROPHYSICAL JOURNAL, 497:824–832, 1998 April 20

THE NEAR-INFRARED INTERSTELLAR SILICATE BANDS AND GRAIN THEORIES

JOHN S. MATHIS
Department of Astronomy, University of Wisconsin- Madison, 475 North Charter Street, Madison, WI 53706; mathis@madraf.astro.wisc.edu
Received 1997 March 4; accepted 1997 November 26

ABSTRACT

With nonporous spherical grains, the interstellar 9.7 and 18 μm silicate bands are observed to be too strong to be compatible with laboratory silicates if the interstellar medium has an abundance of heavy elements that is substantially less than solar, as indicated by a number of recent observations. The dilemma can be resolved if the silicate grains are composite, fluffy, with $\geq 25\%$ vacuum, and spheroidal with axis ratios greater than 2. The presence of carbon in the composite grains does not affect the silicate features much, but vacuum is important.

General problems of grain models are discussed. The strong possibility that the interstellar medium has a composition with a heavy element content less than solar is briefly reviewed, and the importance of interstellar sulfur is emphasized, since it might provide a reason for believing that the interstellar medium has a solar composition. It is shown that there is a fundamental problem regarding providing the 2175 Å feature via any form of carbon: if the aromatic carbon transition in this wavelength region is strong, the central wavelength and form of the feature are sensitive to the shape distribution of the grains, or to the size distribution and states of ionization of polycyclic aromatic hydrocarbons (PAHs) or similar hydrocarbons. If the transition is weak, such as in more disordered carbon ("amorphous" carbon or material resembling coal), then the transition is independent of size and shape distributions, but too much C is required. The general viability of composite (fluffy) grains is considered in the light of recent criticism, and two unresolved problems with the silicate features are mentioned.

Subject headings: dust, extinction — infrared: ISM: lines and bands — ISM: abundances

1. INTRODUCTION

Draine and Lee (1984, hereafter DL) matched the extinction of the diffuse interstellar medium (ISM) over the wavelength range $0.1\ \mu\text{m} \leq \lambda \leq 1000\ \mu\text{m}$, including the strengths of the 9.7 and 18 μm "silicate" features, with the Mathis, Rumpl, & Nordsieck (1977, hereafter MRN) size distribution. The profile of the 9.7 μm band was fitted to the emission in the Trapezium region of the Orion Nebula (Forrest, Gillett, & Stein 1975). DL expressed concern that the strength of the band needed to fit observations was rather large, given the constraints of cosmic abundances of Si, Fe, and Mg. From laboratory estimates of the total band strengths of amorphous silicates, Tielens & Allamandola (1987) suggested that $\sim 150\%$ of the solar abundance of Si in the interstellar medium (ISM) is needed to provide the observed band strength.

Several papers (see, e.g., Snow & Witt 1995, 1996; Mathis 1996, hereafter M96) have discussed the strong evidence that the overall abundance of heavy elements in the ISM, relative to H and He, is appreciably less than solar, perhaps $Z_{\rm ISM}/Z_\odot \approx 0.7$. Recently Cardelli & Meyer (1997) have added krypton to the list of elements indicating a low $Z_{\rm ISM}/Z_\odot$. In addition, observations (Cardelli et al. 1996) have found an abundance of carbon in the gas phase that amounts to $\text{C/H} = (140 \pm 20)$ ppm (parts per million: atoms of C per 10^6 H), as compared to the solar abundance of 360 ppm. The reduction in the amounts of all heavy elements available, and of carbon especially, produces a major challenge for theories of dust that will eliminate many previous models.

M96 has constructed models that deal with the size distribution of the large grains, which contain most of the mass, and finds that the ultraviolet and visual extinction laws can be fitted within the abundance constraints, including the carbon in the gas, down to about $Z_{\rm ISM}/Z_\odot \approx 0.85$ within the commonly accepted values of $A(V)/N(\text{H})$. Inhomogeneous grains, with amorphous carbon (AMC), probably partially hydrogenated, mixed with silicates, are required to explain the observed extinction per H atom with the minimum abundance of refractory elements. In addition, the grains must be somewhat porous, with $\gtrsim 25\%$ of the volume as vacuum. The width of the interstellar polarization law requires that the vacuum fraction not exceed about 60% (Wolff, Clayton, & Meade 1993).

Porous or fractal grains are good interstellar grain candidates, because similar (but larger) specimens are collected as interplanetary dust particles, and because coagulation in dense interstellar clouds must take place.

Inspired by the very low bulk densities shown by radio studies of micrometeroids, Bohren & Wickramasinghe (1977) calculated the cross section of fluffy grains by means of an effective medium theory (EMT) in which the optical behavior of a grain containing of two or more constituents is calculated for a fictitious homogeneous particle of the same shape with a suitably averaged index of refraction. Bohren & Wickramasinghe averaged the optical constants by means of the "Garnett Rule" (Garnett 1904).[1] In the recent past porous grains have been considered by many authors (e.g., Wright 1987, 1989; Mathis & Whiffen 1989; Hage & Greenberg 1990; Ossenkopf 1993; Wolff et al. 1994; Stognienko, Henning, & Ossenkopf 1995), and their optical properties have been computed with increasingly refined numerical techniques.

The strength of the silicate features, not addressed in M96, will be the main focus of this paper. In § 2 the present models, very similar to those in M96, are discussed. Observations and results presented in § 3. Grain models in general are considered in § 4, with emphasis on the form of carbon

[1] Usually called the "Maxwell Garnett Rule," for which Henning & Stognienko (1996) pointed out the correct reference (Maxwell was Dr. Garnett's given name).

that is responsible for the 2175 Å feature. The last section contains final remarks.

2. OBSERVATIONS AND MODELS OF THE SILICATE FEATURES

2.1. *Observations*

The values of $A(V)/\tau(9.7\ \mu m)$, the profile of the near-infrared (NIR) silicate bands, are not easily determined, even from *Infrared Space Observatory* (*ISO*) observations, because the background continuum of the source spectrum must be estimated between about 6 and 30 μm. It is important to observe the absorption profiles of the 9.7 μm bands in objects with no circumstellar silicate features, such as carbon-rich Wolf-Rayet stars (WCs). Using these, Roche & Aitken (1984) found $A(V)/\tau_{9.7} \approx 18$. Whittet (1992, p. 150) suggests 18.5 ± 1.5. From *ISO* data van der Hucht et al. (1996) gives values of $\tau_{9.7}$ for six WCs. However, in WCs the interstellar silicate band is seen against the emission of warm circumstellar carbon grains whose intrinsic profile is not readily apparent. For three stars, the background emission is still rising with wavelength on the short side of the 9.7 μm band, making the interpolation of the continuum difficult, because one must guess where the maximum in the circumstellar emission would be in the absence of the silicate bands. The best WCs, WR 98A and WR 118, have a continuum on both sides of the 9.7 μm band that can be drawn with relatively little ambiguity. For them, van der Hucht et al. (1996) give $A(V)/\tau_{9.7} = (20.4, 19.4)$, respectively. The average of all six WCs is 17.7. The lowest values are in the stars for which it is most difficult to estimate the continuum.

Bowey, Adamson, & Whittet (1998) obtained observations of the 9.7 μm bands in Cyg OB2 no. 12 (also known as VI Cyg no. 12) and three stars in the Taurus cloud. Cyg OB2 no. 12 is seen through an ISM that is considered diffuse, since it shows a very weak or missing ice band (Sandford et al. 1991; Whittet et al. 1997) and $R = 2.90 \pm 0.15$ (Adamson, Whittet, & Duley 1990), which is quite typical for the diffuse ISM in spite of the large extinction per parsec. Cyg OB2 no. 12 also shows a relatively narrow 9.7 μm band that is well fitted by the profile of μ Cephei (Roche & Aitken 1984; Bowey et al. 1997). From *ISO* observations of Cyg OB2 no. 12, Whittet et al. (1997) found $\tau_{9.7} = 0.54 \pm 0.06$; $A(V) = 10.2 \pm 0.3$ mag (Humphreys 1978), so $A(V)/\tau_{9.7} = 10.2/0.54 = 18.9 \pm 2.2$.

I adopt the average of the two best WCs (van der Hucht et al. 1996) and Cyg OB2 no. 12 to obtain $A(V)/\tau_{9.7} = 19.3$. Probably there is enough variation in the details of the bands between various lines of sight within the diffuse ISM that a more precise estimate is not practical. The profile was taken from Roche & Aitken (1984) and Bowey et al. (1997). For estimating the band strength per H atom I use $N(H)/E(B-V) = 5.8 \times 10^{21}$ cm^{-2} mag^{-1} (Bohlin, Savage, & Drake 1978), and $A(V)/E(B-V) = 3.1$.

The only observations of NIR polarization to date are from sources within dense clouds: the BN object in the Orion molecular cloud (Aitken, Smith, & Roche 1989) and AFGL 2591 (Aitken et al. 1988). The profiles are broader than those in the diffuse ISM.

2.2. *Models*

We will consider near-infrared (NIR; here 6–30 μm) opacity and polarization of grains. The size distribution is unimportant, since almost all grains in the diffuse ISM are in the "Rayleigh limit," with sizes much smaller than the relevant wavelengths, and the cross section per gram is independent of the size.

The parameters of each model are (*a*) f_{vac}, the fraction of vacuum assumed in the composite grain; (*b*) the amount of AMC per H atom, usually taken to be 105 ppm, about the minimum required to provide the observed amount of visual extinction per H atom (M96); and (*c*) the $Z_{ISM}/Z_{\odot}$ assumed, which determines the abundances available. All of the available Si was assumed to be in silicates (but see § 4.3 for further discussion of this point.)

Optical constants of AMC in the present range of wavelengths are available for only "glassy," "Be 1," and "AC 1" AMC (Rouleau & Martin 1991.) There is little difference ($\sim$5% of silicate band strength) among the types with published optical constants. The silicates considered are the suite of amorphous pyroxenes ([Mg, Fe] SiO_3) and amorphous olivines ([Mg, Fe]$_2$ SiO_4) by Dorschner et al. (1995) as well as the DL "astronomical silicate." Models with some of the Si in SiO_2 were also considered. The abundances of Mg, Fe, and Si were taken from Anders & Grevesse (1989). The Fe and Mg remaining from the available mixture were assumed to be in the form of $Mg_{0.6}Fe_{0.4}O$ and FeO, whose constants were taken from Henning et al. (1995). Most models included 105 ppm of carbon in the large grains (M96).

With the assumed components, the average optical constants of the grain were calculated using each of three types of EMT (Ossenkopf 1991): (*a*) the simple "Bruggeman rule" (Bohren & Huffman 1983), (*b*) the rule suggested by Ossenkopf (Ossenkopf 1991, Stognienko, Henning, & Ossenkopf 1995), and (*c*) the Garnett Rule. After the dielectric constants were calculated by the EMTs, the extinction and polarization cross sections for spheres and oblate spheroids of 2:1 and 4:1 axial ratios were determined from standard formulae (Bohren & Huffman 1983) for small grains.

Henning & Stognienko (1993) have studied the effects of grain shapes and fractions of vacuum on the 9.7 and 18 μm absorption and polarization profiles using the DL optical constants. They compared silicate band cross sections determined from an EMT to those from the discrete dipole approximation (DDA), which is computationally much more intensive. They found that for nonporous oblate spheroids with a 2:1 axial ratio the EMT cross section is about 5% smaller at the maximum; for 60% vacuum, the difference is 17%. Wolff et al. (1994, and references therein) discussed comparisons of EMTs and the DDA calculations for fluffy grains not in the Rayleigh limit ($2\pi a/\lambda \geq 0.5$) and found excellent agreement if the void sizes were in the Rayleigh limit. For this paper the use of one or more EMTs is dictated by the computing requirements of many models with various parameters.

I take the grain cross sections to be given by the geometric mean of those predicted by the Bruggeman and Ossenkopf rules, which usually differ by 10%–20%. Which rule is larger varies with the material and f_{vac}. The Garnett Rule usually gives a cross section $\approx$15% larger. The choice of average constants is dictated by a DDA calculation of the cross section kindly performed by M. Wolff (1997, private communication) for $\lambda = 9.4$ μm, $f_{vac} = 0.3$, "Be 1" AMC (Rouleau & Martin 1991), and the olivine $Mg_{0.8}Fe_{1.2}SiO_4$. Small random inclusions of each material were included within particles assumed to be spheres or oblate spheroids

with axial ratios of 2:1 and 4:1. His cross sections were very close to those calculated by my recipe.

2.3. *Underlying Continuous Opacity*

Observations of the silicate features refer to the *excess* of the silicate opacity over the continuous opacity, so models must do the same. An extrapolation is required for the underlying continuum opacity of the models $\tau_{\rm cont}(\lambda)$ from about 7.5 μm to longer wavelengths, mainly only to 9.7 μm. The base continuum was written as

$$\tau_{\rm cont}(\lambda) = \tau(6\ \mu{\rm m})(\lambda/6\ \mu{\rm m})^{-F(\lambda)}\ . \quad (1)$$

The $F(\lambda)$ for the models for $6 \leq \lambda(\mu{\rm m}) \leq 7.5$, where the silicate feature is not important, is $\sim$0.5. The exponent $F(\lambda)$ was usually taken to vary linearly with λ:

$$F(\lambda) = 0.5[1 + (\lambda - 6\ \mu{\rm m})/7\ \mu{\rm m}]\ , \quad (2)$$

so that $F(\lambda) = 0.5$ at 6 μm, 1.0 at 13 μm, and 1.5 at 20 μm. The use of equation (2) increases the 9.7 μm silicate band extinction by only about 3% over the simple $F = 0.5$. Several approximations might affect the estimated band strength more than this amount.

At $\lambda \sim 20$ μm, equation (2) predicts that the base is about 10% of the extinction; a simple power law with $F = 0.5$ predicts $\sim$30%. The observational determination of the base is very difficult, subjective, and dependent upon the wavelength interval available for interpolation. Similarly, there is no way to estimate the excess extinction in the minimum between the 10 and 20 μm features, at about 13 μm, from the "underlying continuum" (if there is one). I was forced to adopt the extrapolation.

3. RESULTS

3.1. *Extinction*

Figure 1*a* is a plot of $\tau(\lambda)$ of various models relative to the observed maximum extinction assuming $A(V)/\tau_{\rm max} = 18.9$ and $N({\rm H})/A(V) = 1.9 \times 10^{21}$ cm^{-2} mag^{-1}. A value of unity for the maximum of a model implies that it can just produce the required 9.6 μm extinction. All of the models in the figure have $Z_{\rm ISM}/Z_\odot = 0.85$ and C/H = 105 ppm in the grains (enough to explain the visual extinction per H atom). Figure 1*b* is a similar plot with an expanded wavelength scale that shows the Roche & Aitken (1984) observations (*points*) over their entire range. (The same type of line is used for a particular model in both Figs. 1*a* and 1*b*.)

The solid lines show the model with the largest maximum extinction. It uses amorphous $Mg_{0.8}Fe_{1.2}SiO_4$ 4:1 oblate spheroids and 50% vacuum and provides 1.02 times as much absorption as needed. However the FWHM (see Fig. 1*b*) is $\sim$2.65 μm, as compared to the observed $\sim$2.35 μm. The 18 μm bump has a maximum at 21 μm with a rather flat-topped profile (see further discussion below) with a peak $\sim$70% of that at 9.7 μm.

The short-dashed line in Figure 1*a* shows 4:1 oblate spheroids and 50% vacuum with Draine (1985) "astronomical silicate." This model is like the solid line, except for having DL olivine in place of $Mg_{0.8}Fe_{1.2}SiO_4$. The profile is too broad and is displaced to longer wavelengths. These problems are not surprising: the Draine constants were developed for use with compact spheres, in which case DL showed that they fitted the NIR profile very well.

The dotted lines show the model with the best pyroxene, Mg SiO_3, along with 50% vacuum in 4:1 spheroids. The model can just explain the $Z_{\rm ISM}/Z_\odot = 0.85$ silicate band strength with a width of about the observed value.

The dot-dashed curve in Figure 1*a* shows the effects of changing from $f_{\rm vac} = 0.5$ to compact grains. Otherwise, the model is the same as for the solid line ($Mg_{0.8}Fe_{1.2}SiO_4$, 4:1 spheroids.) The maximum extinction has been significantly reduced, especially at 18–20 μm. However the maximum

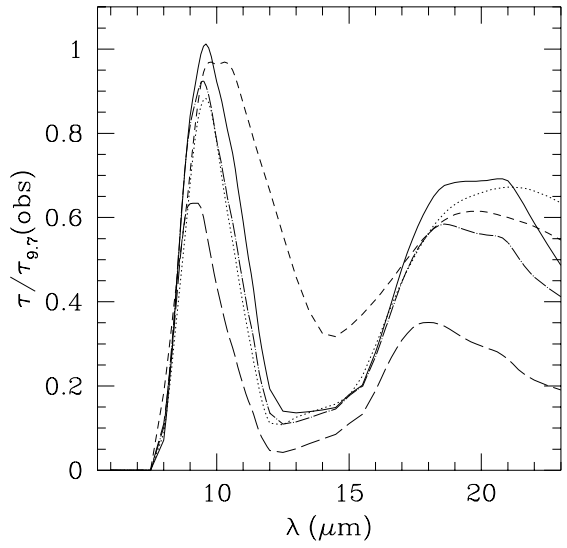

FIG. 1*a*

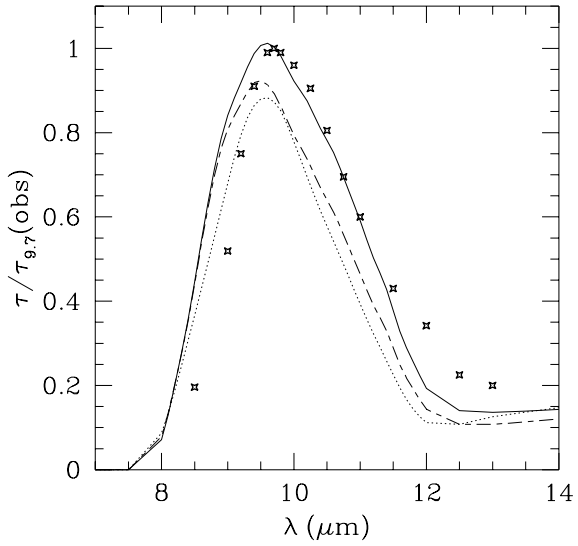

FIG. 1*b*

FIG. 1.—(*a*) Extinction of various models $\tau(\lambda)$ relative to $\tau_{9.7}$(obs), the maximum observed silicate band extinction per $A(V)$, plotted against wavelength. All models contain C/H = 105 ppm in amorphous carbon and assume $Z_{\rm ISM}/Z_\odot = 0.85$. A value of unity at the maximum of a curve means that it can just fulfill the silicate extinction requirements. *Solid line:* Amorphous olivine ($Mg_{0.8}Fe_{1.2}SiO_4$) with $f_{\rm vac} = 0.5$, oblate spheroids with 4:1 axial ratio. *Dotted line:* Amorphous pyroxene Mg SiO_3, $f_{\rm vac} = 0.5$, 4:1 spheroids. *Dot-dashed line:* $Mg_{0.8}Fe_{1.2}SiO_4$ 4:1 spheroids with $f_{\rm vac} = 0$. *Short-dashed line:* Draine (1985) "astronomical" silicate with $f_{\rm vac} = 0.5$ in 4:1 oblate spheroids. *Long-dashed line:* $Mg_{0.8}Fe_{1.2}SiO_4$ with $f_{\rm vac} = 0$ and spheres. (*b*) Extinction of models relative to the maximum observed, as in Fig. 1*a*. All models have 105 ppm of AMC and $Z_{\rm ISM}/Z_\odot = 0.85$. *Points:* Observations of Roche & Aitken (1984). *Solid line:* As in Fig. 1*a*: amorphous $Mg_{0.8}Fe_{1.2}SiO_4$, $f_{\rm vac} = 0.5$, 4:1 oblate spheroids. *Dotted line:* Mg SiO_3, $f_{\rm vac} = 0.5$, 4:1 spheroids. *Long-dash–short-dashed line:* $Mg_{0.8}Fe_{1.2}SiO_4$ $f_{\rm vac} = 0.5$, spheres.

strength is still enough to explain plausibly the observed strength, considering the uncertainty in the values of $A(V)/\tau_{9.7}$ ($\pm 10\%$) and of the EMTs. This profile is almost exactly the same as for $Mg_{0.8}Fe_{1.2}SiO_4$ spheres with 50% vacuum (not shown). Changing from oblate spheroids to spheres or from olivines to Mg SiO_3 reduces the extinction by $\sim 10\%$ at 9.7 μm and by even less at 20 μm if grains are kept fluffy.

The bottom curve in Figure 1*a* shows $Mg_{0.8}Fe_{1.2}SiO_4$ grains that are both compact and spherical. The maximum extinction is reduced to well below the requirement. Other types of silicates all show the same result.

Figure 1*b* shows an additional model: the long-dash–short-dashed line is the model with $Mg_{0.8}Fe_{1.2}SiO_4$ 50% vacuum and spheres instead of spheroids (*solid line*). It is about the same as compact grains with spheroids. It is the combination of $f_{vac} = 0$ and spherical grains that produces the low-absorption model shown in Figure 1*a*.

Figure 2 shows the extinction of models, normalized to the maximum value of each curve in order to emphasize the profiles. The observations (Roche & Aitken 1984) are the points. The light solid line is for $Mg_{0.8}Fe_{1.2}SiO_4$ with $f_{vac} = 0.5$ and 4:1 spheroids. The dotted line shows the same grains with Mg SiO_3 silicate. The profiles are similar, but the width of the Mg SiO_3 is closer to the observations.

The 2:1 spheroids have extinction maxima 6%–8% lower than is shown in Figure 1 for 4:1 spheroids. Spheres are 2% lower still. At the 18 μm maximum, the 4:1 spheroids absorb 15% more than 2:1 spheroids and 19% more than spheres. For compact grains, the shape effect is even larger; 4:1 spheroids have 45% larger absorption than spheres at the 9.6 and 18 μm maxima. The polarization produced by the 4:1 spheroids is 81% larger than for the 2:1 grains.

Not shown are the effects of varying the type of AMC. The "AC1" AMC models corresponding to the light solid lines would lie $\sim 3\%$ below those in Figure 1 at 9.7 μm and 10% below at 20 μm, with the maximum occurring at 19 μm and being flatter than in Figure 1*a*. Similar effects occur for the other cases.

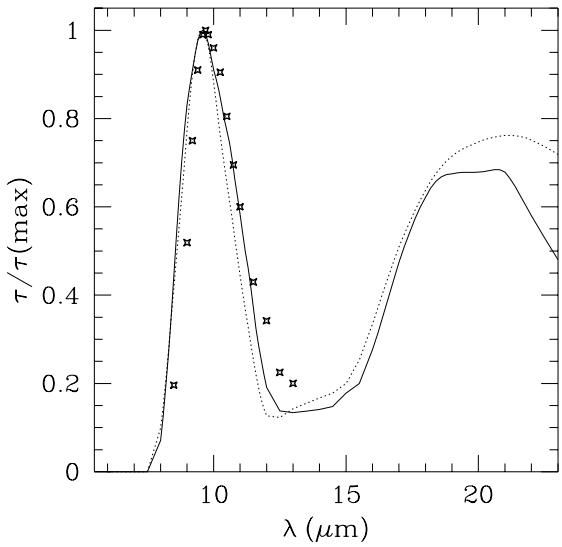

FIG. 2.—Extinction curves normalized to their maximum values, showing their profiles. *Points:* Observed extinction (Roche & Aitken 1984). Models had $f_{vac} = 0.5$ and used C/H = 105 ppm. *Solid line:* Models from 4:1 oblate spheroids of $Mg_{0.8}Fe_{1.2}SiO_4$. *Dots:* Mg SiO_3, the best pyroxene in terms of producing extinction.

Some of the results in this section were also obtained by Henning & Stognienko (1993) using the Draine (1985) silicate. These models considered other amorphous silicates.

The maximum NIR band strength increases about 16% when going from no AMC in the 4:1 spheroids to 105 ppm. The AMC, if in separate carbonaceous grains, would contribute nothing to the silicate band. This increase in band strength is crucial in understanding the band strength for reduced ISM abundances. The type of AMC is not important for increasing the NIR band strengths, but it does affect the visual albedo and visual extinction per H atom (M96).

For olivines, the 9.6 μm absorption is 85% of the maximum at $f_{vac} = 0$, $\geq 97\%$ for $0.25 \leq f_{vac} \leq 0.65$, and 93% for $f_{vac} = 0.8$. The lowering of the absorption for $f_{vac} = 0$ grains is significant, but other values of f_{vac} are effectively unconstrained by the strengths of the silicate bands.

The wavelength of the maximum occurs at 9.5–9.6 μm for all shapes and degrees of vacuum considered here ($f_{vac} \leq 0.8$). The wavelength of the maximum τ_{18} is shifted from 18.8 to 20.8 μm as the oblateness increases from spheres to 4:1 spheroids, with or without vacuum. For DL silicates the maximum occurred at 18.8 μm. Henning & Stognienko (1993) found maxima at 18.7–19.0 μm, using the DDA approximation with differing amounts of vacuum and graphite inclusions.

Models with glassy SiO_2 instead of silicates, and (Fe, Mg) also in oxides, provide very poor fits to the silicate features. The motivation for considering such models arises from gas-phase abundances of Si, Fe, Mg (Fitzpatrick 1996, and references therein; see § 4.3.) The models have very strong narrow bands peaking at 9.2 μm, not 9.7 μm, if the amount of Si in SiO_2 is ≥ 0.15. With less SiO_2 there is a shoulder at 9.2 μm.

In summary, laboratory silicates can produce enough absorption to meet the observational requirements, if the grains are somewhat fluffy and contain carbon. As Figure 1 shows, if $Z_{ISM}/Z_\odot \lesssim 0.9$, the silicate band strength serves as a diagnostic for grain models, but is not as challenging as $A(V)/N(H)$.

3.2. *The* 18 μm *Band*

The 18 μm extinction is poorly determined because of the difficulty in estimating the background continuum as well as the low opacity. Whittet (1992, p. 147) suggests $\tau(18\ \mu m)/\tau_{9.7} = 0.4$. Toward the Galactic center $\tau(18)/\tau(9.7) \geq 0.6$ (McCarthy et al. 1980). Even with data from space, there will probably be serious problems in determining the underlying continuum at these wavelengths.

The olivine models that fit the 9.7 μm feature best ($f_{vac} = 0.5$) have $\tau_{18}/\tau_{9.7} = 0.7$ for $Mg_{0.8}Fe_{1.2}SiO_4$ and 0.57 for Mg Fe SiO_4. The extinction is almost constant between 18 and 22 μm. Nonporous grains have $\tau_{18}/\tau_{9.7} = 0.44$ for Mg Fe SiO_4 but insufficient strength at 9.7 μm. The pyroxenes have ratios of $\tau_{18}/\tau_{9.7}$, similar to olivines.

4. COMMENTS ON GRAIN MODELS

This paper has explained the strengths of the silicate bands in terms of composite fluffy grains similar to those discussed in M96. There are other grain models, including the "standard" MRN model of DL, compact silicate-core grains with organic refractory mantles (Greenberg & Li 1996; Li & Greenberg 1997), the models containing poly-

cyclic aromatic hydrocarbons (PAHs) and "very small grains" plus large grains (Désert, Boulanger, & Puget 1990; Siebenmorgen & Krügel 1992; Dwek et al. 1997), or empirically determined size distributions of compact grains (Kim & Martin 1995; Kim, Martin, & Hendry 1994). With solar abundances or slightly below, all models explain the interstellar extinction and polarization laws with suitably chosen alignment rules for the large grains.

I believe that the two main issues confronting grain models are the composition of the ISM and the form that carbon takes in the ISM. They are related: if (and only if) there is plenty of carbon (i.e., almost solar), the observations can be explained in a variety of ways. If $Z_{\rm ISM}/Z_\odot \lesssim 0.9$, with 140 ppm of C in the gas (Cardelli et al. 1996), the carbon must be used very efficiently to account for the 2175 Å bump, the NIR emission bands and continuum, the extended red emission (ERE), and the optical extinction beyond what is possible with silicates or oxides alone. With a solar C/H = 355 ppm (Grevesse, Noels, & Sauval 1996) and $Z_{\rm ISM}/Z_\odot = 0.8$, the total abundance of carbon in the dust is $(0.8 \times 355 - 140) = 144$ ppm, far below that used by any current grain model except M96.[2] With more generous solar C/H estimates, for example, ~ 400 ppm (e.g., Anders & Grevesse 1989, with a 1 σ increase), there are 180 ppm of C available, which is still a major challenge. There is plenty of carbon in the largest suggested solar abundance (Meyer 1988), 490 ± 120 ppm, but such a large abundance seems improbable.

4.1. *The Composition of the ISM*

The basis for suspecting that abundances in the ISM are subsolar has three independent lines of reasoning to support it (M96):

1. The gas-phase O/H in the diffuse ISM (Meyer et al. 1994; Sofia, Cardelli, & Savage 1994; Meyer, Jura, & Cardelli 1997) is accurately determined and is coupled with the measurement of the very low abundances of water ice, O_2, and CO. The ISM abundances of N, Ar, and Kr are also subsolar.

2. Abundances of young stars as determined from stellar atmospheres are generally subsolar. Snow & Witt (1996) give average abundance for B stars, but there is a considerable spread among the various determinations. An assessment of the systematic errors is badly needed to make this result convincing.

3. Abundances of H II regions in the solar vicinity are almost always subsolar (e.g., Simpson et al. 1995; Afflerbach, Churchwell, & Werner 1997), based on standard abundance analyses. In planetary nebulae, the effects of inhomogeneities with significant differences of temperature and/or density from the average is strongly suggested by major discrepancies in the abundances of C^{+2} and O^{+2} as determined from recombination lines and collisionally excited lines. However Esteban et al. (1998) find that the very faint recombination lines in the Orion Nebula have excess strengths at only about the 1 σ level. The Orion abundances of O, N, and Ne are about 0.2 dex below solar even after a correction for temperature fluctuations is applied. *If the N and O abundances in the ISM are solar, then there must be serious errors in the standard abundance determinations from stellar atmospheres and* H II *regions, including virtually all extragalactic determinations.*

Perhaps the best evidence *against* a low $Z_{\rm ISM}/Z_\odot$ in the ISM comes from the element S, which seems to be undepleted relative to solar in the ISM (see a discussion by Fitzpatrick & Spitzer 1996). There are interesting implications if even one element in the ISM has a solar gas-phase abundance relative to H. Either (*a*) the ISM is enriched in that element relative to the others (or the Sun is deficient); (*b*) the observations, either solar or ISM, are wrong (perhaps because of *f* values); or (*c*) the proper ISM abundance is solar, and the other elements are really depleted. Since O and S are both produced in Type II supernovae, it seems difficult to believe that only S could be enriched in the ISM or depleted in the primordial solar nebula. If the interstellar S/H is solar, all of the problems discussed above remain. More work is needed to find [S/H] in the ISM.

If the abundances of O, N, and other elements in the ISM are subsolar, *and if the ratios of* Fe, Mg, *and* Si *to* O *and* N *are solar*, then the extra absorption provided by fluffy composite grains seems necessary. The direct measurement of the ISM abundances (gas and dust combined) of Fe, Si, and Mg seems very difficult because of the unknown amounts contained in dust, unless X-ray halos can possibly be used as diagnostics.

4.2. *What Form Does Carbon Take in the Diffuse ISM?*

Carbon is by far the most abundant of the refractory elements and must be responsible for much of the interstellar absorption and emission. It must contribute at least the bulk if not all of several phenomena: the unidentified infrared bands (UIBs: emission bands with 3.28 μm $\leq \lambda \leq$ 18.02 μm), the NIR emission continuum for $\lambda \leq 30$ μm, the extended red emission, the 2175 Å feature, much of the optical extinction on every grain model, and probably much of the extinction for $\lambda \leq 0.16$ μm. These statements come from the low abundances of all refractory elements when O and N are eliminated by observed spectra. Models must make the most economical use of all forms of carbon to explain all of these phenomena. So far, no model has done so.

4.2.1. *The* 2175 Å *Feature and Emissions from Carbonaceous Grains*

The 2175 Å feature (the excess of the extinction law near 220 nm above a smoothly drawn underlying continuum, integrated over the profile) has been attributed to graphite (MRN/DL; Siebenmorgen & Krügel 1992; M96; Li & Greenberg 1997); PAHs (e.g., Joblin, Léger, & Martin 1992), PAH derivatives (Beegle et al. 1997), very small grains (Désert et al. 1990); quenched carbonaceous composite, a carbonaceous residue (Sakata et al. 1994); and material similar to anthracite coal (Papoular et al. 1996), which has given an excellent review of the forms of carbon that might be producing the bump. Blanco et al. (1996) have shown that *all* laboratory measurements of the bump in actual materials provide a feature that is too broad to fit the narrowest observed interstellar profiles and at the wrong central wavelength for spherical particles. The latter objec-

[2] Li & Greenberg (1997) require C/H = 194 ppm, 93% of solar. Their suggestion of lowering the C requirement by assuming 20% lower densities for the constituents while keeping the optical constants the same is equivalent to an arbitrary increase of the cross sections over the laboratory values.

tion could be met by changing the assumed shape. This procedure seems to involve no more fine-tuning than assuming spherical grains, which are excluded by interstellar polarization as well.

In the following I will discuss a rather fundamental conundrum: If the bump is caused by a very strong absorption requiring a small amount of carbon, its profile and wavelength must depend upon the shape (or distribution of shapes) of the solid or upon the size and shape of the molecule containing that carbon. If the bump is a relatively weak transition because of disorder within the aromatic carbons in the grains, the bump profile does not depend greatly on the geometrical arrangement of the carbons, but an unacceptably large amount of carbon is required to produce it.

The observations of the bump (see Mathis 1994 for a review and references) that make it difficult to interpret are mainly the very low spread (± 9 Å; Fitzpatrick & Massa 1988) in the values of its central wavelength and a variation in its FWHM from 0.80–1.20 μm^{-1} for stars outside of quiescent dark clouds.

To understand why there is either a shape dependence for the grains producing the bump or else a large carbon requirement, we must consider the physics of the absorption. The bump is almost surely produced by absorption in $\pi - \pi^*$ orbitals of the shared electron within the benzene rings of aromatic C of radiation with its electric vector parallel to the plane of the rings. We will assume that the carriers of the bump are small (size $\ll \lambda/2\pi$), since otherwise both the central wavelength and the width of the feature depends upon the size distribution of carriers. The question is, in what form are the assemblies of benzene rings in space? If the C is "amorphous," the planar rings are in domains of ~ 10 Å in size,[3] surrounded by C with diamondlike (tetrahedral) bonding or jumbled C atoms (plus other elements in interstellar grains). In this case there is little or no bump because of the perturbations of the neighboring C atoms on the $\pi - \pi^*$ orbitals. If the C is well ordered in sheets of benzene rings, without many imperfections for several 10s of Å, there is a strong collective $\pi - \pi^*$ resonance. I will call this material "graphite," although that term really implies perfect order that is unimaginable in grains. Intermediate ranges of order, such as in high-grade coal or some deposited carbons, produce the bump, but more weakly than graphite does. PAHs are planar sheets of rings that have their $\pi - \pi^*$ resonance somewhat affected through the peripheral boundary conditions (including the H atoms attached,) so each PAH has unique structure in its 200–240 nm absorption.

The strength of the $\pi - \pi^*$ absorption influences the dielectric constant $\epsilon(\lambda) \equiv \epsilon_1 + i\epsilon_2$. The absorption acts somewhat like a classical oscillator with a maximum in ϵ_2 at the resonant frequency and a minimum in ϵ_1 that can be less than zero at a somewhat higher frequency. The cross section σ of any small ellipsoidal particle is given by (Bohren & Huffman 1983)

$$\frac{\sigma}{V} = \frac{2\pi}{\lambda} \frac{\epsilon_2}{(1 - L + L\epsilon_1)^2 + L^2\epsilon_2^2}, \quad (3)$$

where V is the volume of the particle and L ($0 \le L \le 1$) depends strongly upon the shape of the ellipsoid along each principal axis, with the σ being appropriate for radiation with the electric vector oriented along that axis. If the $\pi - \pi^*$ absorption is strong enough to make $\epsilon_1 < 0$, there is an L such that $\epsilon_1 = -(1/L - 1)$. In this case equation (3) shows that the $L\epsilon_1$ term in the denominator vanishes. This condition is called a "surface plasmon resonance." There is a particular shape corresponding to the resonant L for either prolate or oblate spheroids. Since ϵ_1 depends upon wavelength, the resonance wavelength changes with L or with shape. This condition is the major weakness for assigning the bump to graphite, as discussed by Gilra (1972), M96, and Rouleau, Henning, & Stognienko (1997). The objection pertains to any model that produces the bump by making the term containing $L\epsilon_1$ become small, thereby making σ/V become large. In graphite the resonance is strong because ϵ_2 is rather small at the resonance, making σ large.

Equation (3) shows that σ/V does not involve the grain size, unlike the distribution of larger grains (e.g., DL; MRN) in which both the size distribution and shapes must be invariant for various lines of sight.

The $\pi - \pi^*$ resonance in aromatic carbon causes a decrease in the value of ϵ_1 around the range 200–250 nm. For AMCs, $\epsilon_1 \sim 2$–3 at 300 and 150 nm; some AMCs show a decrease near 250 nm, but ϵ_1 is always positive, so there is no strong increase in σ/V near 220 nm. As the $\pi - \pi^*$ absorption increases with increasing order in the arrangement of the C atoms, the minimum value of ϵ_1 decreases. With the DL constants for graphite, ϵ_1 reaches a minimum of -3.36, but the maximum σ/V occurs when $\epsilon_1 \sim -1.3$, mainly because of the wavelength dependence of ϵ_2. Graphite can produce the bump with C/H $\sim$ 50–60 ppm, with about the correct width ($\sim$0.8–1.1 μm^{-1}) and central wavelength, provided the laboratory constants are modified somewhat from those in DL, which in turn are somewhat different from the actually measured ones. Of course, astronomical graphite is subject to impurities and processing that require it to differ from the pure graphite analyzed in the laboratory.

Explaining the variations in the width of the bump with graphite is difficult, but I think that the problems are no worse than those using PAHs or other forms of C (see below). Coatings of a PAH-like material of various thickness might be able to broaden the bump without shifting it, if a considerable amount of fine-tuning is allowed (Mathis 1994). The bump is narrowest in H II regions, where such coatings might be minimal, and broadest in the dark quiescent regions, as predicted by this idea.

Neutral PAHs, with their well-ordered (planar) benzene rings, have $\pi - \pi^*$ absorptions per C that have about the same strength (or f value) as graphite when integrated over wavenumber, judging from ovalene ($C_{32}H_{14}$; Leach 1995, quoting Joblin 1992) and mixtures of PAHs (Joblin et al. 1992; see also Dartois & d'Hendecourt 1997). The average oscillator strength f per C atom is $\sim$0.19, about the same as the DL constants give for graphite flakes with random orientation. Thus PAHs, whose presence is shown by the UIBs, will surely contribute to the bump, but they seem to be unsuitable for explaining the bump by themselves (see below).

The problems of explaining the bump entirely with PAHs include (*a*) the shape of the absorption; (*b*) the invariance of the central wavelength of the bump; and (*c*) the ionization

[3] The C atoms within the benzene ring are 1.42 Å apart, and the planes of rings in graphite are separated by 3.37 Å.

of PAHs to anions and cations, which should vary among the many lines of sight that have been observed.

If the bump is caused by mixtures of PAHs, the laboratory measurements of those molecules, if appropriate to the gas phase, must be used without modification. Impurities are not appropriate for modifying the optical constants, as they (perhaps) are for the laboratory constants of pure graphite.

The $\pi - \pi^*$ feature is too broad ($\sim 1.2\ \mu m^{-1}$) even for the single PAH ovalene (Leach 1995). The simplest PAH, naphthalene ($C_{10}H_8$; Salama & Allamandola 1992) has a feature that is narrow enough but with considerable structure and an unsuitable central wavelength. Mixtures of PAHs (Joblin et al. 1992) produce too broad a bump and show a shoulder at ~ 3000 Å that would seem difficult to mask (see also Salama, Joblin, & Allamandola 1995 for relative profiles of two other PAHs also showing a great deal of structure). The PAH absorption would have to be averaged over many species to give the smooth profile seen in space, so the observed invariance of the central wavelength in various directions would have to be explained by a mixture of PAHs that averages to a smooth extinction law, with a maximum at 2175 Å and without the shoulder near 300 nm that appears in PAH spectra, while broadening the profile symmetrically about the maximum by differing amounts. Such a distribution of PAHs seems very improbable to me, while graphite can meet most of these criteria.

The PAH idea is further weakened by the fact that PAHs probably exist as anions, neutrals, and cations in space (Dartois & d'Hendecourt 1997, and references therein.) The 220 nm PAH feature is weakened in cations (Lee & Wdowiak 1993), which also have a feature at ~ 400 nm that is not present in the neutrals or in the extinction law. In summary, it seems that PAHs are at least as problematic as graphite in producing the bump.

Well-ordered carbon similar to coal (Papoular et al. 1996) shows a feature similar to the bump, but the absorption is so weak that ϵ_1 never becomes negative. The advantage of this condition is that the profile and maximum wavelength of the absorption feature do not depend upon the shapes or sizes of the absorbers, within wide limits, because the denominator in equation (3) is almost independent of L. Unfortunately, the denominator is not very small, so the absorption is comparatively weak. Papoular et al. (1996) estimate that the bump requires C/H $\sim$ 230 ppm for the bump using polycrystaline graphite, meaning graphitized carbon but with small domains. This C abundance requires solar C/H for the bump alone. This behavior illustrates the conundrum at the beginning of this section: one can have (*a*) a weak bump insensitive to size and shape distributions, but using too much carbon; or (*b*) a bump with modest abundances (~ 50 ppm for graphite), but with sensitivity to the shape distribution; or (*c*) PAHs, which are about as efficient as graphite but show asymmetric profiles that should be sensitive to distribution of sizes and states of ionizations.

The bump is probably actually produced by *both* graphitic grains and PAHs or more disordered forms of hydrocarbons, with possibly a continuum of sizes and shapes. The PAHs are, of course, indicated by the UIBs. The graphitic grains (not perfect graphite, but perhaps stacked PAHs) would help to make the profile more symmetric and possibly narrower (although this statement requires a leap of faith that is based on the observational evidence). Since both PAHs and graphite produce the bump with about the same strength per C atom, the carbon requirement is about the same as in M96 (~ 50–60 ppm). The quantitative assignment of the bump between PAHs and graphite (which might represent large PAHs) is beyond the scope of this paper.

The strength of the bump is poorly correlated with the extinction law outside of the interval 250 nm $\geq \lambda \geq$ 200 nm (Mathis & Cardelli 1992), especially in the far-UV (Greenberg & Chlewicki 1983). Since PAHs have a rather strong extinction at far-UV wavelengths, they cannot be primarily responsible for both the bump and the far-UV extinction, but they can contribute to both.

The UIBs and extended red emission (ERE; Witt 1989; Witt & Boroson 1990) are probably explained adequately by the PAHs and hydrogenated amorphous carbon (HAC) that are needed to explain the bump and visual extinction, respectively. *COBE* has filter observations over the range 3.5–1000 μm (Dwek et al. 1997) showing that $\sim 25\%$ of the Galactic diffuse emission is from the UIBs and underlying NIR continuum. This radiation would be contributed by the UV absorption of the bump particles and PAHs that are absorbing the far-UV radiation.

The C requirement of the ERE depends upon the fluorescence yields and radiation field of the material giving rise to the emission (see Furton & Witt 1993). Tielens et al. (1996) suggest that C/H $\sim$ 30 ppm of HAC explains the ERE. This material could be in composite fluffy grains that need C/H $\sim$ 100 ppm to provide the visual extinction, so I find that the ERE is not a major challenge to grain models. It has also been suggested that PAHs can provide the ERE (d'Hendecourt et al. 1986).

4.2.2. *Can Fluffy Grains Provide the NIR Emission?*

Dwek (1997) criticized composite fluffy grain models in M96, seemingly in general, on the basis of its neglect of PAHs and the model with the minimum carbon requirements absorbing too much energy in the optical/UV. E. Dwek (1997, private communication) and I have agreed that (*a*) the excellent *COBE* observations provide a new integral involving the energy absorbed at optical/UV wavelengths and reradiated in the NIR/FIR; (*b*) the application of the FIR test involves estimating the relatively uncertain UV and optical interstellar radiation field times the otherwise unobserved absorption (in contrast to extinction) of the grains; and (*c*) the objections of Dwek (1997) apply to the model in M96 using the particular "Be 1" form of AMC and not necessarily to composite fluffy grain models in general. Other models in M96 that use carbon and that scatter more in the optical/UV, of which there are several (see Table 1 in M96), seem promising in meeting the FIR test as well as reduced cosmic abundances (though not as low as "Be 1"). Lowering the optical interstellar radiation field and increasing the UV will also produce the same effect as increasing the grain albedo.

PAHs were not considered explicitly in M96 because of the estimates by Pendleton et al. (1994) and Tielens et al. (1996) that PAHs contain $\sim 1\%$ of solar C (4 ppm); Sandford (1996, Table 1) suggests a range of 2%–10% of solar C (7–36 ppm). Dwek et al. (1997) estimate that 70 ± 20 ppm of C is needed in PAHs to explain the 4–30 μm emission bands and continuum. These wildly different estimates illustrate the difficulty of determining PAH cross sections (compare Désert et al. 1990 and Joblin et al. 1992) and the

strengths of the UIBs above the underlying continuum that is contributed in part by the cooling of the stochastically heated small grains (graphite in M96).

Li & Greenberg (1997) have suggested that composite grain models cannot be correct, because the grains would not be stable against rotation if they are only held together by van der Waals forces, the weakest of molecular interactions with energies of $\sim 10^{-3}$ eV. Chemical bonds, responsible for cementing the small particles in composite grains such as interplanetary dust particles (e.g., Brownlee 1978) that were collected by aircraft have energies of ~ 1 eV, so the criticism seems to have limited validity.

Optical polarization is not as much a test of grain models as it is of alignment mechanisms, since fluffy grains with $\lesssim 50\%$ vacuum provide polarization that fits the observed polarization law (Wolff et al. 1993). The fitting of the optical extinction with reduced C/H ratios is a much more stringent test.

4.3. *Further Problems That Have Not Been Addressed*

One problem related to the 2175 Å feature is the formation of well-ordered carbon from the amorphous material ejected by carbon stars and how dehydrogenation affects the bump (Blanco et al. 1996). Menella et al. (1996) have studied the effects of UV radiation on small AMC grains and find a growth of the bump, but the final product, after exposure to much less radiation than an interstellar grain would suffer, is still far from graphite.

There are two other general problems that have not been adequately addressed by any current grain models:

1. What causes the gas-phase abundance patterns of Fe, Mg, and Si observed along several lines of sight? The observations (Sofia et al. 1994; Savage & Sembach 1996; Fitzpatrick 1996) show that about half of the Si is returned to the gas phase in some low-density comoving structures ("clouds"), along with only 10% of the Fe and Mg. In these clouds each Si atom cannot be combined with even one atom of (Fe, Mg) in a silicate. The pattern of abundances is present at all radial velocities, so it is not likely to be some isolated phenomenon. The straightforward explanation is that most of the Si, Mg, and Fe might be in oxides rather than within the same silicate molecule, but the present models indicate that such oxides would not produce silicate NIR features like those observed.

2. How is SiC oxidized to silicate? Carbon-rich stellar ejecta comprise $\sim 50\%$ of the input into the ISM; Whittet, Duley, & Martin (1990) have concluded from an upper limit on the 11.15 μm line of SiC that at most 5% of Si is in SiC, the dominant form of Si in carbon-rich objects. This paper has used $Z_{\rm ISM}/Z_\odot$ times the entire solar abundance in the silicates, so that the SiC, a very refractory material, has been converted to silicates. Perhaps SiC is not bonded tightly to carbonaceous grains in circumstellar outflows, so that the SiC grains are separate and are vaporized by interstellar shocks, and the subsequent gaseous Si is oxidized after it condenses onto grain surfaces.

5. DISCUSSION AND SUMMARY

We have seen that the strength of the 9.7 μm silicate band above the underlying continuous absorption can be explained with $Z_{\rm ISM}/Z_\odot = 0.8$, assuming compact fluffy grains, the laboratory optical constants of glassy olivine silicates, and EMTs to derive cross sections. Pyroxenes seem appreciably less promising. Carbon and fluffiness in composite silicate grains increases the strengths of the NIR bands above the underlying continuum.

There are technical problems involved in predicting the NIR extinctions. These models used the average of two EMTs on the basis of a DDA calculation by M. Wolff, but the errors depend upon the individual values of the dielectric constants of each material at each wavelength. Even an exact calculation of a particular grain geometry necessarily involves rather arbitrary assumptions about the geometry of each grain constituent, including the voids. Systematic errors in the EMT approach might be 20% or more. There is clearly a limit of grain models to predict the observations. Perhaps the true elemental abundances of the ISM will become known, as well as measurements by means of IR absorption and emission band strengths of the amounts of specific candidate materials. The use of laboratory optical constants of pure materials is not really appropriate, since there is strong processing of grains within the ISM. At present models can only try to show gross characteristics of grains. Probably whether they are fluffy or not is one such feature.

In regard to whether interstellar grains are porous or not, an old line of reasoning (Mathis & Whiffen 1989; Ossenkopf 1993) seems worth repeating: how can the ISM *avoid* forming composite fluffy grains? The basic observations are (*a*) that a large fraction of some elements (Fe, Mg, Ti, etc.) is in the solid form, judging from their gas-phase abundances (Jenkins 1987; Crinklaw, Federman, & Joseph 1994), and (*b*) that the extinction law in dense regions, with large values of R, is lower in the ultraviolet (UV) than extinction in the diffuse ISM. The low gas-phase abundances of refractory elements show that the evolution is primarily a rearrangement of solids rather than vaporization and condensation from the gas phase; there is not enough gaseous material to coat the small grains with ices so that they become large in comparison to UV wavelengths. The lack of small grains in dense regions must be caused by coagulation into larger ones. How can one coagulate the many small grains onto large ones and keep the resulting grain with chemically separated components? How can small grains be packed into large ones without there being substantial amounts of vacuum within the agglomerate? O'Donnell & Mathis (1996) found that the MRN-like size distribution is established by the shattering of large composite grains into a distribution of smaller sizes by collisions with smaller grains in the low-density ISM, but the aggregation of smaller grains into large composites takes place on a rapid timescale within dense clouds. Jones, Tielens, & Hollenbach (1996) have shown that shattering of large monolithic grains (≥ 0.1 μm) into smaller ones must take place rapidly in comparison with the average age of material in the ISM, so large compact grains cannot survive long enough unless they are somehow grown within the ISM like large composites. There are large grains in meteorites: graphite (e.g., Bernatowicz et al. 1996) and SiC (e.g., Hoppe et al. 1994), but their cosmic-ray exposure ages are only $\sim 10^8$ yr (Lewis, Amari, & Anders 1994).

Explaining the properties of grains will continue to be a challenge for the foreseeable future, but ongoing observations are allowing progress.

This research has been partially supported by NASA. J. S. M. greatly appreciates the DDA calculations by M.

Wolff for oblate silicates grains and has benefited considerably from friendly correspondence with E. Dwek. The DDA computations utilized the Cray C90 at the Pittsburgh Supercomputing Center under proposal number AST 92-0002P (M. Wolff, P. I.). The paper was improved by a thoughtful referee report.

REFERENCES

Adamson, A. J., Whittet, D. C. B., & Duley, W. W. 1990, MNRAS, 243, 400
Afflerbach, A., Churchwell, E. B., & Werner, M. W. 1997, ApJ, 478, 190
Aitken, D. K., Roche, P. R., Smith, C. H., James, S. D., & Hough, J. 1988, MNRAS, 230, 629
Aitken, D. K., Smith, C. H., & Roche, P. F. 1989, MNRAS, 236, 919
Anders, E., & Grevesse, N. 1989, Geochim. Cosmochim. Acta, 53, 197
Beegle, L. W., Wdowiak, T. J., Robinson, M. S., Cronin, J. R., McGeehee, M. D., Clemett, S. J., & Gillette, S. 1997, ApJ, 487, 976
Bernatowicz, T. J., Cowsik, R., Gibbons, P. C., Lodders, K., Fegley, B., Jr., Amari, S., & Lewis, R. S. 1996, ApJ, 472, 760
Blanco, A., Fonti, S., Muci, A. M., & Orofino, V. 1996, ApJ, 472, 419
Bohlin, R. C., Savage, B. D., & Drake, J. F. 1978, ApJ, 224, 132
Bohren, C. F., & Huffman, D. R. 1983, Absorption and Scattering of Light by Small Particles (New York: Wiley)
Bohren, C. F., & Wickramasinghe, N. C. 1977, Ap&SS, 50, 461
Bowey, J. E., Adamson, A. J., & Whittet, D. C. B. 1998, MNRAS, in press
Brownlee, D. E. 1978, in Protostars and Planets, ed. T. Gehrels (Tucson: Univ. Arizona Press), 134
Cardelli, J. A., & Meyer, D. M. 1997, ApJ, 477, L57
Cardelli, J. A., Meyer, D. M., Jura, M., & Savage, B. D. 1996, ApJ, 467, 334
Crinklaw, G., Federman, S. R., & Joseph, C. L. 1994, ApJ, 424, 748
Dartois, E., & d'Hendecourt, L. 1997, A&A, 323, 534
Désert, F. X., Boulanger, F., & Puget, J. L. 1990, A&A, 237, 215
d'Hendecourt, L. B., Léger, A., Olofsson, G., & Schmidt, W. 1986, A&A, 170, 91
Dorschner, J., Begemann, B., Henning, Th., Jäger, C., & Mutschke, H. 1995, A&A, 300, 503
Draine, B. T. 1985, ApJS, 57, 587
Draine, B. T., & Lee, H. M. 1984, ApJ, 285, 89 (DL)
Dwek, E. 1997, ApJ, 484, 779
Dwek, E., et al. 1997, ApJ, 475, 565
Esteban, C., Peimbert, M., Torres-Peimbert, S., & Escalante, V. 1998, MNRAS, in press
Fitzpatrick, E. L. 1996, ApJ, 473, L55
Fitzpatrick, E. L., & Massa, D. 1988, ApJ, 307, 286
Fitzpatrick, E. L., & Spitzer, L., Jr. 1996, ApJ, 475, 623
Forrest, W. J., Gillett, F. C., & Stein, W. A. 1975, ApJ, 195, 423
Furton, D. G., & Witt, A. N. 1993, ApJ, 415, L51
Garnett, J. C. M. 1904, Philos. Trans. R. Soc. London, A, 203, 385
Gilra, D. P. 1972, in The Scientific Results of the *Orbiting Astronomical Observatory OAO-2*, ed. A. D. Code (Washington, DC: NASA SP-310), 295
Greenberg, J. M., & Chlewicki, G. 1983, ApJ, 272, 563
Greenberg, J. M., & Li, A. 1996, A&A, 309, 258
Grevesse, N., Noels, A., & Sauval, A. J. 1996, in Cosmic Abundances, ASP Conf. Ser. 99, ed. S. S. Holt & G. Sonneborn (San Francisco: ASP), 117
Hage, J. I., & Greenberg, J. M. 1990, ApJ, 361, 251
Henning, Th., & Stognienko, R. 1993, A&A, 280, 609
———. 1996, A&A, 311, 291
Henning, Th., Begemann, B., Mutschke, H., & Dorschner, J. 1995, A&AS, 112, 143
Hoppe, P., Amari, S., Zinner, E., & Lewis, R. S. 1994, ApJ, 430, 870
Humphreys, R. M. 1978, ApJS, 38, 309
Jenkins, E. B. 1987, in Interstellar Processes, ed. D. J. Hollenbach & H. A. Thronson (Dordrecht: Reidel), 533
Joblin, C. 1992, Ph.D. thesis, Univ. Paris
Joblin, C., Léger, A., & Martin, P. 1992, ApJ, 393, L79
Jones, A. P., Tielens, A. G. G. M.,& Hollenbach, D. J. 1996, ApJ, 469, 740
Kim, S.-H., & Martin, P. G. 1995, ApJ, 444, 293
Kim, S.-H., Martin, P. G., & Hendry, P. D. 1994, ApJ, 422, 164
Leach, S. 1995, Planet Space Sci., 43, 1153
Lee, W., & Wdowiak, T. J. 1993, ApJ, 410, L127
Lewis, R. S., Amari, S., & Anders, E. 1994, Geochim. Cosmochim. Acta, 58, 471
Li, A., & Greenberg, J. M. 1997, A&A, 323, 566
Mathis, J. S. 1994, ApJ, 422, 176
———. 1996, ApJ, 472, 643 (M96)
Mathis, J. S., & Cardelli, J. A. 1992, ApJ, 398, 610
Mathis, J. S., Rumpl, W., & Nordsieck, K. H. 1977, ApJ, 217, 425 (MRN)
Mathis, J. S., & Whiffen, G. 1989, ApJ, 341, 808
McCarthy, J. F., Forrest, W. J., Briotta, D. A., & Houck, J. R. 1980, ApJ, 242, 965
Mennella, V., Colangeli, L., Palumbo, P., Rotundi, A., Schutte, W., & Bussoletti, E. 1996, ApJ, L191
Meyer, J.-P. 1988, in Origin and Distribution of the Elements, ed. G. J. Mathews (Singapore: World Scientific), 337
Meyer, D., Jura, M., & Cardelli, J. A. 1997, ApJ, 493, 221
Meyer, D. M., Jura, M., Hawkins, I., & Cardelli, J. A. 1994, ApJ, 437, L59
O'Donnell, J. E., & Mathis, J. S. 1996, ApJ, 479, 806
Ossenkopf, V. 1991, A&A, 251, 210
———. 1993, A&A, 280, 617
Papoular, R., Conard, J., Guillois, O., Nenner, I., Reynaud, C., & Rouzaud, J.-N. 1996, A&A, 315, 222
Pendleton, Y. J., Sandford, S. A., Allamandola, L. J., Tielens, A. G. G. M., & Sellgren, K. 1994, ApJ, 437, 683
Roche, P. F., & Aitken, D. K. 1984, MNRAS, 208, 481
Rouleau, F., & Martin, P. G. 1991, ApJ, 377, 526
Rouleau, F., Henning, Th., & Stognienko, R. 1997, A&A, 322, 633
Salama, F., & Allamandola, L. J. 1992, ApJ, 395, 301
Salama, F., Joblin, C., & Allamandola, L. J. 1995, Planet. Space Sci., 43, 1165
Sandford, S. A. 1996, Meteoritics & Planetary Science, 31, 449
Sandford, S. A., Allamandola, L. J., Tielens, A. G. G. M., Tapia, M., & Pendleton, Y. 1991, ApJ, 371, 607
Sakata, A., Wada, S., Onaka, T., & Tokunaga, A. T. 1987, ApJ, 320, L63
Savage, B. D., & Sembach, K. R. 1996, ARA&A, 34, 279
Siebenmorgen, R., & Krügel, E. 1992, A&A, 259, 614
Simpson, J. P., Colgan, S. W. J., Rubin, R. H., Erickson, E. F., & Haas, M. R. 1995, ApJ, 444, 721
Snow, T. P., & Witt, A. N. 1995, Science, 270, 1455
———. 1996, ApJ, 468, L65
Sofia, U. J., Cardelli, J. A., & Savage, B. D. 1994, ApJ, 430, 650
Stognienko, R., Henning, Th., & Ossenkopf, V. 1995, A&A, 296, 757
Tielens, A. G. G. M., & Allamandola, L. J. 1987, in Interstellar Processes, ed. D. J. Hollenbach & H. A. Thronson, Jr. (Dordrecht: Reidel), 403
Tielens, A. G. G. M., Wooden, D. H., Allamandola, L. J., Bregman, J., & Witteborn, F. C. 1996, ApJ, 461, 210
van der Hucht, K., et al. 1996, A&A, 315, L193
Whittet, D. C. B. 1992, Dust in the Galactic Environment (Bristol: IOP)
Whittet, D. C. B., Duley, W. W., & Martin, P. G. 1990, MNRAS, 244, 427
Whittet, D. C. C. B., et al. 1997, preprint
Witt, A. N. 1989, in IAU Symp. 135, Interstellar Dust, ed. L. J. Allamandola and A. G. G. M. Tielens (Dordrecht: Kluwer), 87
Witt, A. N., & Boroson, T. A. 1990, ApJ, 355, 182
Wolff, M. J., Clayton, G. C., Martin, P. G., & Schulte-Ladbeck, R. 1994, ApJ, 423, 412
Wolff, M. J., Clayton, G. C., & Meade, M. R. 1993, ApJ, 403, 722
Wright, E. L. 1987, ApJ, 320, 818
———. 1989, ApJ, 346, L89